Geophysical Research Letters

RESEARCH LETTER
10.1029/2022GL101950

Key Points:

- A significant warming trend in sea surface temperature at the genesis of tropical mesoscale convective systems (MCSs) sea surface temperature threshold (SST_G) has been observed
- A global climate model that can explicitly simulate MCSs captures the observed features of SST_G and projects a continuous increase
- A constant relationship between SST_G and upper-tropospheric temperature indicates the existence of a moist-adiabatic adjustment

Supporting Information:

Supporting Information may be found in the online version of this article.

Correspondence to:

W. Dong,
Wenhao.Dong@noaa.gov;
wenhaodong2015@gmail.com

Citation:

Dong, W., Zhao, M., Ming, Y., & Ramaswamy, V. (2022). Significant increase in sea surface temperature at the genesis of tropical mesoscale convective systems. *Geophysical Research Letters*, *49*, e2022GL101950. https://doi.org/10.1029/2022GL101950

Received 31 OCT 2022
Accepted 18 NOV 2022

Significant Increase in Sea Surface Temperature at the Genesis of Tropical Mesoscale Convective Systems

Wenhao Dong[1,2], Ming Zhao[2], Yi Ming[2], and V. Ramaswamy[2]

[1]Cooperative Programs for the Advancement of Earth System Science, University Corporation for Atmospheric Research, Boulder, CO, USA, [2]NOAA/Geophysical Fluid Dynamics Laboratory, Princeton, NJ, USA

Abstract An event-based assessment of the sea surface temperature (SST) threshold at the genesis of tropical mesoscale convective systems (MCSs) is performed in this study. We show that this threshold (SST_G) has undergone a significant warming trend at a rate of ~0.2°C per decade. The SST_G shows a remarkable correspondence with the tropical mean SST and upper-tropospheric temperature on interannual and longer timescales. Using a high-resolution global climate model that permits realistic simulations of tropical MCSs, we find that the observed features of SST_G are well simulated. Both observation and model simulations demonstrate that the upward tendency in SST_G primarily results from the environmental SST warming over MCS genesis regions rather than the changes in MCS genesis location. A continuous increase in SST_G is projected in a warming simulation, but the relationship between SST_G and upper-tropospheric temperature remains unchanged, suggesting that the tropical tropospheric temperature generally follows a moist-adiabatic adjustment.

Plain Language Summary The development of tropical ocean showers and thunderstorms requires a warm ocean surface as an energy source fueling the storm. As a good example, a sea surface temperature (SST) threshold of 26.5°C has long been recognized as a necessary condition for tropical cyclone genesis. Here we examine the SST threshold at the genesis of tropical mesoscale convective systems, which occur so frequently throughout the tropics that they play an important role in shaping the general circulation of the atmosphere as they redistribute moisture and energy in the atmosphere. Using satellite observations and a high-resolution global climate model, we show that this threshold has undergone a significant warming trend during the past several decades and will continue to increase in the future. This warming trend is closely related to the changes in the tropical mean SST. A constant relationship between the SST threshold and upper-tropospheric temperature is found in both the current climate and a warming climate, which corroborates the argument that tropospheric temperatures in the tropics approximately follow a moist adiabatic adjustment.

1. Introduction

The occurrence of tropical deep convection, including tropical cyclones (TCs) and mesoscale convective systems (MCSs), is observed above an sea surface temperature (SST) threshold falling in the vicinity of 25°C~28°C for the present climate (Dare & McBride, 2011; Defforge & Merlis, 2017a, 2017b; Evans & Waters, 2012; Graham & Barnett, 1987; Johnson & Xie, 2010; Tompkins, 2001; Tory & Dare, 2015). Though the precise value of this threshold has been a matter of debate (McTaggart-Cowan et al., 2015), the consensus is that these convective systems generally occur more frequently and with stronger intensities over warmer SSTs. The SST threshold for cyclogeneses has been extensively analyzed due to their reliable and sufficiently long observational track records. A warming trend in SST at the time of TC genesis was observed although the magnitude of the trend varies in those studies (Dare & McBride, 2011; Defforge & Merlis, 2017a). However, TCs only account for a small fraction of tropical deep convection, as there are approximately 80 times more tropical deep convection events than TC events (Defforge & Merlis, 2017a). Johnson and Xie (2010) made use of the monthly rainfall to estimate the SST required for the more general tropical deep convection. They found an increasing trend of this SST threshold at a rate of about 0.1°C per decade during 1980–2009. And this upward trend of the convection threshold was projected to continue in the future based on the Coupled Model Intercomparison Project Phase 3 (CMIP3) simulations. Similar results have been found based on a set of warming scenarios that span a wide range of CO_2 concentrations (Evans & Waters, 2012). These warming simulations demonstrated that the critical SST for tropical convection, estimated using monthly outgoing longwave radiation, increases as the climate warms.

Here we analyze the event-based SST at the genesis of tropical (defined as areas within 30° of the equator) MCSs. As the largest form of cumulonimbus cloud complex, MCSs develop when convection aggregates and grows upscale, forming mesoscale circulation that organizes the convection (Houze, 2004, 2018; Moncrieff, 2004; Moncrieff & Liu, 2006). They occur so frequently throughout the tropics that they play an important role in shaping the general circulation of our climate systems through the production of abundant rainfall and redistribution of energy in the atmosphere (Houze, 2018). MCSs are also common ingredients of various climate extreme events that cause weather-related hazards in the tropics (Doswell et al., 1996; Kunkel et al., 2012; McCollum et al., 1995). It is therefore of interest to examine the evolution of SST at the genesis of MCSs and its potential response to a warming climate. By using a multi-year satellite observation and a new high-resolution global climate model (C192AM4) developed at the Geophysical Fluid Dynamics Laboratory, we show that there is a significant warming trend (~0.2°C per decade) in the SST threshold for the occurrence of tropical MCSs. This upward trend is slightly larger than changes in the tropical mean SST, and it is primarily a result of temporal changes in the environmental SST rather than changes in the location of MCS genesis. The C192AM4 can well capture the observed interannual variability and long-term trend of this SST threshold, and a warming scenario simulation suggests the upward trend will continue in the future. The robust relationship between this SST threshold and upper-tropospheric temperature noted in the current climate is found to persist in a warming future, indicating that the tropical atmosphere will follow a moist-adiabatic adjustment as climate warms.

2. Materials and Methods

2.1. MCS and SST Data Sets

Tropical MCSs identified and tracked in Dong et al. (2021) for both the observation and the C192AM4 model are used in this study. The adopted MCS tracking algorithm was detailed in Huang et al. (2018). Here is a brief summary of this two-step algorithm. It first identifies MCS candidates based on a brightness temperature (T_b) threshold and a minimum area coverage threshold, which are set to 233 K and 5,000 km^2, respectively, in this study. After initial identification, a tracking procedure is performed to link those identified objects. Candidates in consecutive timeframes with more than 15% overlapping area are classified as the same MCS. For those small or fast-moving MCSs when no sufficient overlapping between two timeframes, the tracking procedure invokes a Kalman Filter approach to provide an estimate for the movement of potential MCSs. A comprehensive comparison between these two data sets was documented in Dong et al. (2021), which showed that the C192AM4 can capture various aspects of the observed tropical MCSs reasonably well, including the spatial distribution, seasonality, and interannual variability of MCS frequency as well as the strong relationship between MCS duration (intensity) and size (i.e., longer-lived and stronger events tend to be bigger). For each identified MCS, its genesis is defined as the first point along its track when the T_b and minimum area coverage thresholds are met. The location of each MCS is defined by its centroid (weighted center of T_b within the identified MCS) rather than all the grid points occupied by this MCS. Results based on all grid points show very similar features of SST_G as those discussed here (figures not shown). This selection is adopted to minimize the potential impacts associated with the MCS size, which has been found to be biased large in the model simulations (Dong et al., 2021). The corresponding SST value is the threshold for the genesis of MCS, shortened as SST_G afterward. The daily Optimal Interpolation Sea Surface Temperature (OISST; Reynolds et al., 2007) at a resolution of 1/4° is matched with observed MCSs. This product was developed using an optimum interpolation technique to merge various satellite observations with in situ measurements. To compensate for the biases in the satellite data (e.g., cloudy or rainy regions), a bias correction using in situ data is applied with the error correlation length scales in the tropics to be about 150–200 km and 3 days (De Meyer & Roca, 2021; Reynolds et al., 2007). To account for these uncertainties, we consider a time lag analysis of SST_G up to 2 days (De Meyer & Roca, 2021; Tory & Dare, 2015). Similar analysis has been done for the model simulations except that the C192AM4 model is driven by the Hadley Centre Sea Ice and Sea Surface Temperature (HadISST; Rayner et al., 2003) data set (See more details of C192AM4 model setup below). Two reanalysis products, the ERA5 (Hersbach et al., 2020) and the NCEP/NCAR Reanalysis 2 (NCEP-R2; Kanamitsu et al., 2002), are used to probe the linkage between SST_G and the upper-tropospheric temperatures.

2.2. C192AM4 Model and Experiment Design

The C192AM4 model is a moderately high-resolution (~50 km) version of the latest GFDL atmospheric GCM AM4 (Zhao et al., 2018a, 2018b). C192 denotes 192 × 192 grid points in each of its six cubed-sphere faces.

This model was used for GFDL's participation in the Coupled Model Intercomparison Project Phase 6 (CMIP6) HighResMIP project (Haarsma et al., 2016). A three-member ensemble of the C192AM4 historical simulations spanning 1950–2014 (referred to as C192AM4-PD) is used to evaluate the simulated SST_G in the present-day climate. They are driven by the observed daily SSTs and sea-ice concentrations, greenhouse gases, and natural and anthropogenic aerosol emissions with slightly different initial conditions. We also examine the SST_G in a warming scenario covering 2015–2050 (referred to as C192AM4-FU). The future SSTs and sea ice concentrations were generated by the ensemble mean of the CMIP5 coupled model projections based on the representative concentration pathway 8.5 (RCP8.5) scenario (Haarsma et al., 2016). The specifications of the future radiative gases and aerosol emissions follow the CMIP6 Shared Socioeconomic Pathways 5 (SSP5). In addition to tropical MCSs, C192AM4 has been found to be able to well represent other features of tropical disturbances, including atmospheric rivers andTCs (Zhao, 2020, 2022). Analysis of the C192AM4-PD simulation covers 1985–2008 to coincide with the observation. While for C192AM4-FU simulation, a same length of 24-year is used when we calculate its difference from C192AM4-PD simulation. This is adopted to reduce the potential biases associated with different sample size though the results do not change if the whole 36-year is used.

2.3. Definition of SST_G^{Env} and SST_G^{Loc}

Changes in the SST_G can arise from both variations in the geographic location of MCS geneses (SST_G^{Loc}) and temporal changes in the environmental SST (SST_G^{Env}). Here, following previous studies (Defforge & Merlis, 2017b; Kossin, 2015), the values of SST_G^{Loc} are obtained by replacing the daily time-varying SSTs with the long-term (climatological) monthly mean SSTs, which are calculated for each grid point and each month by averaging over the overlapping period of 1985–2008 for the observation and C192AM4-PD simulation while 2015–2050 for C192AM4-FU simulation. This choice is to keep the seasonal cycle of SST but remove its interannual variability and long-term trend. The values of SST_G^{Env} are obtained by assigning MCS genesis information (location, day, and month) to a particular year during the period analyzed. For each year, we randomly repeated this process 10 times (equivalent to a total of ∼300,000 MCSs) and averaged the resultant SST_G over the 10 realizations to obtain the value of SST_G^{Env}. This process shuffles the location of MCS genesis and thus removes any trends from potential changes in MCS tracks.

3. Results

3.1. Observed and Simulated Features of SST_G

Consistent with previous studies (Dong et al., 2020; Houze, 2018), frequent MCS geneses are observed over the tropical Indian Ocean and the Warm Pool region (Figure S1 in Supporting Information S1). Additionally, large values are noted over the intertropical convergence zone (ITCZ) and South Pacific convergence zone (SPCZ). The C192AM4-PD simulation captures the observed distribution pattern fairly well, with a centered pattern correlation of 0.89 ($p < 0.001$). The tropical mean bias in the simulated oceanic MCS genesis is −5.1%. The mean SST patterns based on the OISST data set and the HadISST data set show very similar distributions ($r = 0.99$, $p < 0.001$) with only slight differences in the tropical Indian Ocean and the Warm Pool region (Figure S2 in Supporting Information S1).

The observed probability density distribution of SST_G over the entire tropics is negatively skewed, a shape that favors warmer SST (Figure 1a). It clearly shows that the majority of SST_Gs are greater than 26°C, with only 11% of the observed MCSs generated over colder SSTs (Figure 1). This result is consistent with previous studies that show tropical convection is weak and rarely observed over regions where SSTs are less than 26°C (Zhang, 1993). The tropical mean SST_G is about 28°C, two degrees larger than the tropical mean SST (SST_M), with a small seasonality of less than 0.5°C based on OISST (Table S1 in Supporting Information S1). To calculate the spatial distribution of SST_G, we resample the MCS geneses into 5° × 5° latitude-longitude grid boxes. This coarse-graining procedure ensures reasonable sample sizes for each grid and provides robust estimates of SST_G. As shown in Figure 2a, the spatial distribution of SST_G generally corresponds to the mean SST distribution, with larger SST_G observed over the tropical Indian Ocean and the Warm Pool region. But the spatial distribution of SST_G is more flat compared to the mean SST distribution with smaller zonal gradient (Figure S3 in Supporting Information S1). All the above features are well simulated in the C192AM4-PD simulations (Figures 1 and 2;

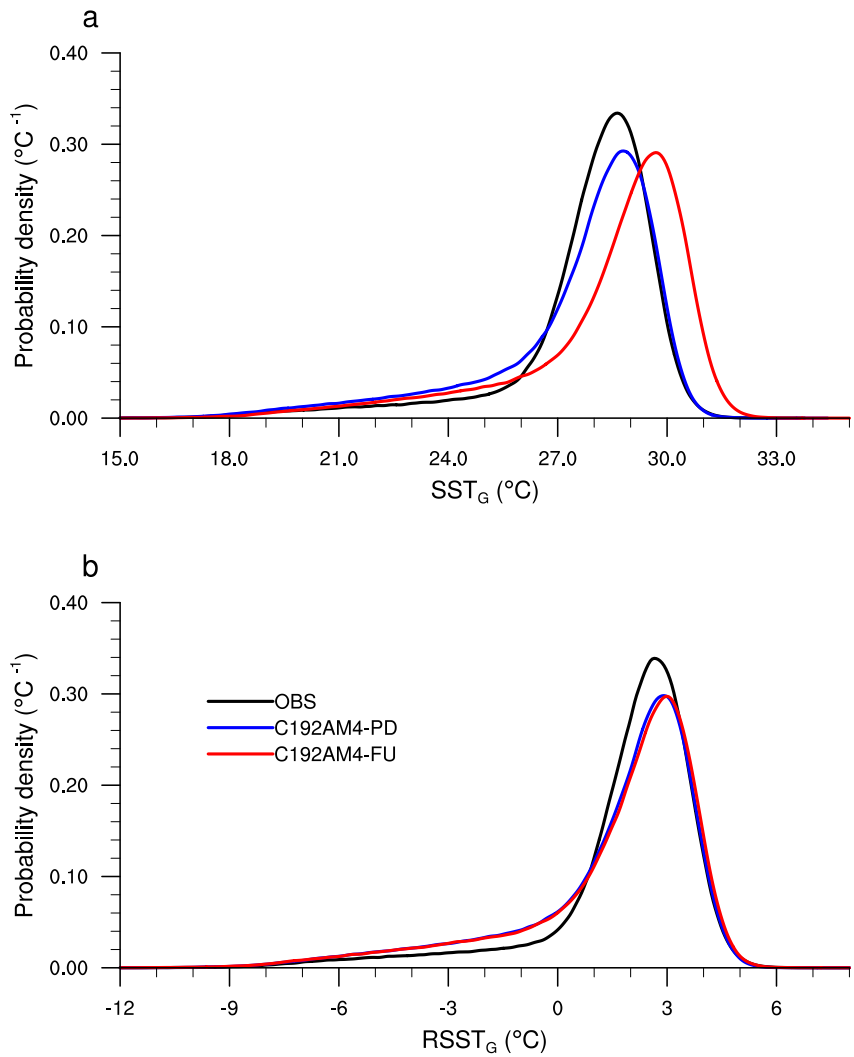

Figure 1. Probability density plot of (a) sea surface temperature (SST) at the genesis of mesoscale convective systems (MCS) (SST_G) and (b) relative SST at the genesis of MCS ($RSST_G$) based on observation (black; 1985–2008), C192AM4-PD (blue; 1985–2008), and C192AM4-FU (red; 1985–2008). The relative SST_Gs are calculated with respect to the corresponding monthly tropical mean SST.

Figure S3 and Table S1 in Supporting Information S1), albeit that they overestimate MCS genesis with SST_G less than 26°C (19%) and the simulated SST_G is slightly larger over the Warm Pool region. Note the difference among the three ensemble members is very small.

Figure 3a shows the observed time series of SST_M and SST_G. Both metrics show significant ($p < 0.05$) positive trends based on the Mann-Kendall test, with the increasing rate to be 0.22°C per decade for SST_G and 0.16°C per decade for SST_M, respectively. The SST_G shows a remarkable correspondence with the SST_M. The interannual correlation coefficient between them after detrending is 0.83 ($p < 0.001$). These values remain almost unchanged if the HadISST data set is used instead of the OISST data set (Figure S4 in Supporting Information S1). The SST_G exhibits substantial variability on shorter timescales as well. It is clear to see variability associated with ENSO events. The C192AM4-PD simulations well reproduce the warming trends of SST_G (0.19°C per decade) and SST_M (0.13°C per decade) as well as a similarly strong correspondence ($r = 0.91$, $P < 0.001$) between these two metrics (Figure 3b).

We replicate the above analysis using the lagged SST to test the robustness of the SST_G features. Both the 1-day lagged and 2-day lagged SST_G (SST_G^{lag1} and SST_G^{lag2}) show almost identical results (mean differences are less than 0.06°C) in terms of the probability density of SST_G and $RSST_G$ despite their respective maximum differences for

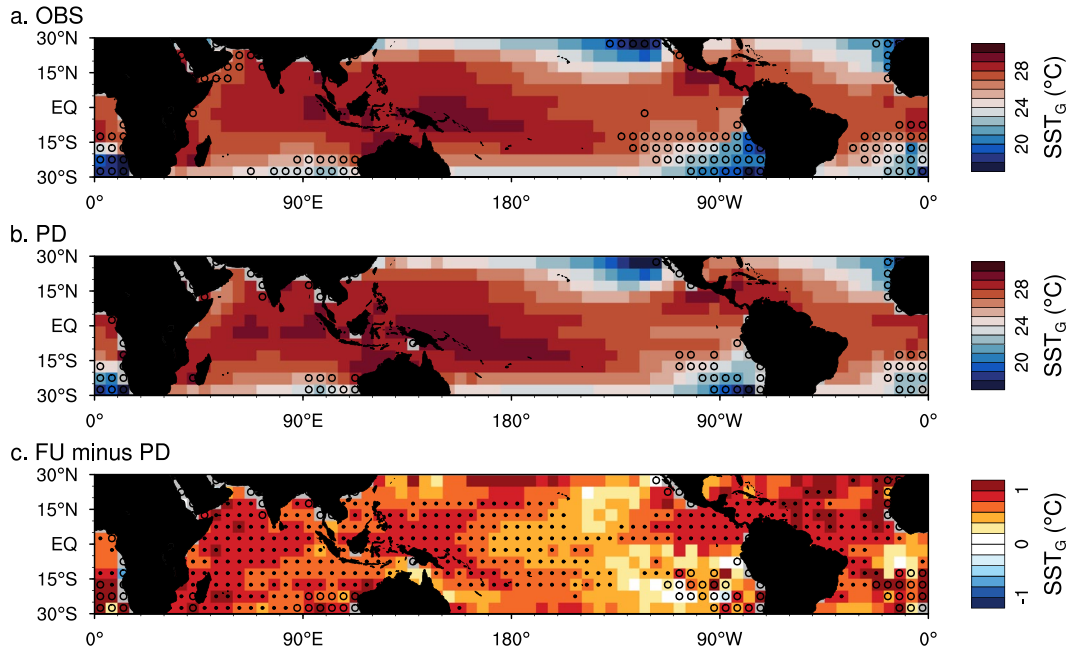

Figure 2. Tropical distribution of the sea surface temperature (SST) at the genesis of mesoscale convective systems (MCS) (SST_G) based on (a) observation and (b) the C192AM4-PD during 1985–2008. (c) The difference between C192AM4-FU (2027–2050) and C192AM4-PD (1985–2008). Circles in (a) through (c) denote grids where sample size are less than 200 while stippling in (c) denotes where differences are statistically significant at the 95% confidence level ($p < 0.05$ based on a two-sided t test).

individual events can be as large as a few degrees (Figure S5 in Supporting Information S1). The impact of the lagged SST on the spatial distribution of SST_G (Figures S6 and S7 in Supporting Information S1) as well as their linear trends (Figure S8 in Supporting Information S1) are also pretty small. This differs from previous studies examining the SST at the genesis of TCs (Tory & Dare, 2015) or SST associated with extreme precipitation (De Meyer & Roca, 2021), which found robust relationships when lagged SST was used. This might be partly attributed to the much larger sample size (>700,000 for both observation and model simulations) analyzed in this study. When the observed change in SST_G is further decomposed into SST_G^{Loc} and SST_G^{Env}, the increasing trend is found to primarily stem from SST_G^{Env} (0.19°C per decade) with a negligible trend of SST_G^{Loc} (0.04°C per decade) (Figure 3d). This indicates that the warming trend of the SST_G is dominated by the changes in environmental SST over the frequent MCS genesis regions rather than the changes in the genesis location of MCSs. Such a characteristic is borne out in the C192AM4-PD simulations (Figure 3e). The simulated linear trends of SST_G^{Loc} and SST_G^{Env} are 0.17°C per decade and 0.01°C per decade, respectively. Similar results are obtained based on the HadISST data set (Figure S4 in Supporting Information S1).

3.2. Dependence of SST_G on the MCS Features

Both the observed and simulated duration, size, and intensity of tropical MCSs have been assessed extensively in our previous study (Dong et al., 2021). Consistent with Roca et al. (2017), all these three key MCS features are found to be highly non-normally distributed. MCSs with shorter duration, smaller size, and weaker intensity largely outnumber those longer-lived, larger and more intense systems. As a result, one may query the results presented here could be biased toward those relatively short-lived, small and weak systems. To probe if SST_G is sensitive to different MCS catalog, we study the dependence of mean SST_G and its linear trend on the MCS duration, size, and intensity, respectively. The observational data set shows a peak-like structure between the mean SST_G and the MCS duration, with the SST_G slightly increasing with the MCS duration prior to 21-hr but decreasing afterward (Figure S9a in Supporting Information S1). A weak though statistically significant ($p < 0.001$) dependence is simulated in the model for both PD and FU simulations, with the increasing rate to be about 0.03°C per 3-hr increase in duration (Figures S9b and S9c in Supporting Information S1). Neither the observed nor the simulated trend of SST_G shows any dependency on the MCS duration. Similarly, the observed

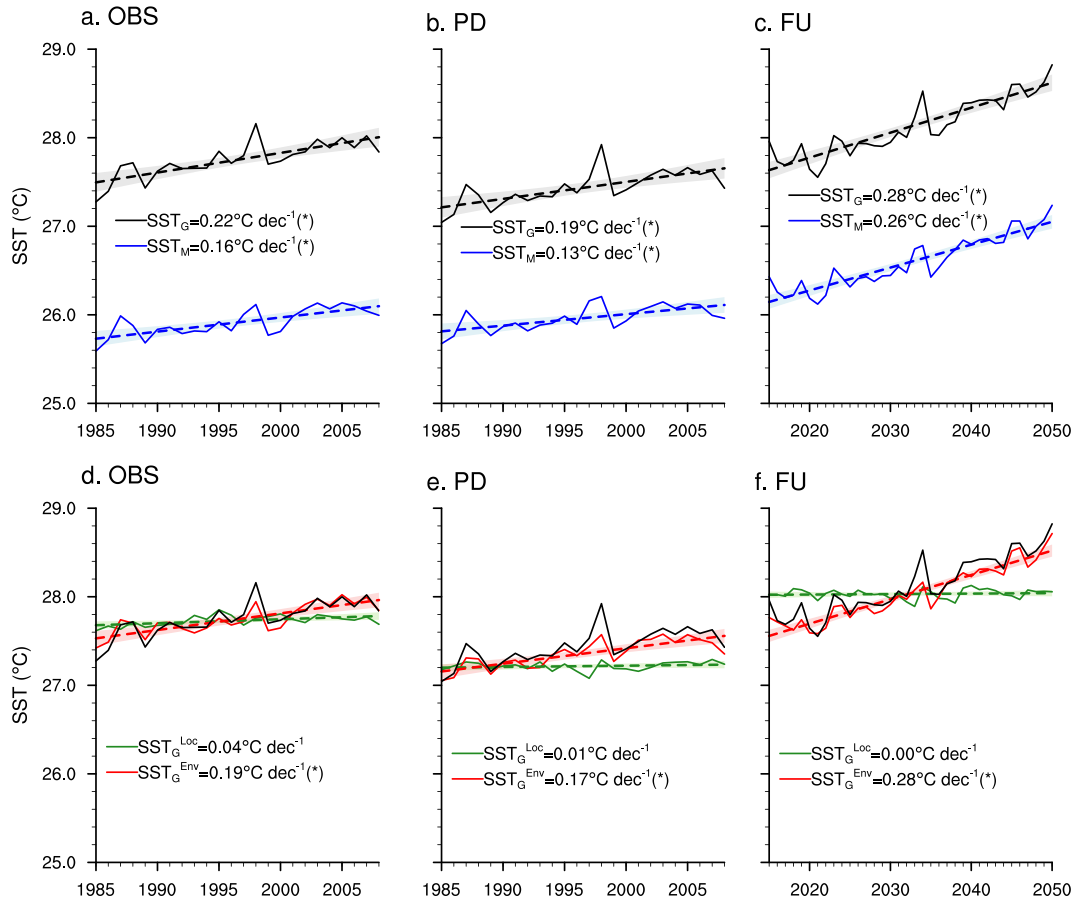

Figure 3. (a–c) Time series of tropical mean sea surface temperature (SST) (SST_M) and SST at the genesis of mesoscale convective systems (MCS) (SST_G) based on (a) observation and (b) C192AM4-PD during 1985–2008, and (c) C192AM4-FU during 2015–2050. (d–f) Same as (a–c) but for SST_G, SST_G^{Env} and SST_G^{Loc}. For each time series, the linear trends (dashed lines) and the 95% confidence intervals (shaded area) are shown. The asterisk indicates that the linear trend is statistically significant at the 95% confidence level.

mean SST_G shows no dependence on the MCS size (Figure S9d in Supporting Information S1) while the dependences simulated by the model for PD and FU simulations (Figures S9e and S9f in Supporting Information S1) are pretty small (0.05°C per 10,000-km^2 increase in size; $p < 0.001$). And no dependence is noted between the SST_G trend and the MCS size for both observation and model simulations. However, for the MCS intensity (third row in Figure S9 in Supporting Information S1), both the observed and simulated mean SST_G demonstrate a strong dependence on the MCS intensity at a similar rate of 0.1°C per 1-K decrease in T_b ($p < 0.001$). Such dependencies are more prominent at lower intensity (i.e., larger T_b values). Moreover, the observed SST_G trend decreases as the MCS intensity increases (0.006°C per dec per 1-K decrease in T_b; $p < 0.001$), but this dependence is not found in model simulations. In summary, the SST_G shows negligible dependences on the MCS duration and size, but it has a strong dependence on the MCS intensity, with stronger MCS corresponding to larger SST_G. The SST_G trends show no dependence on MCS duration and size, but larger trends are observed for weaker systems.

3.3. Response of SST_G to a Warming Climate and Its Implications

The model's considerable skills in simulating tropical MCSs and SST_G during the historical period lend credibility to the model-projected future changes. Based on the C192AM4-FU simulation, the genesis number of tropical MCSs is projected to decrease by 2% with uneven spatial distribution (Figure S1c in Supporting Information S1). Significant decreases are projected over the tropical Indian Ocean, subsidence regions, and Atlantic while increases are projected over the Warm Pool region and tropical Eastern Pacific. By contrast, the spatial distribution of SST_G shows significant increases over nearly all tropical oceanic grids except the subsidence regions

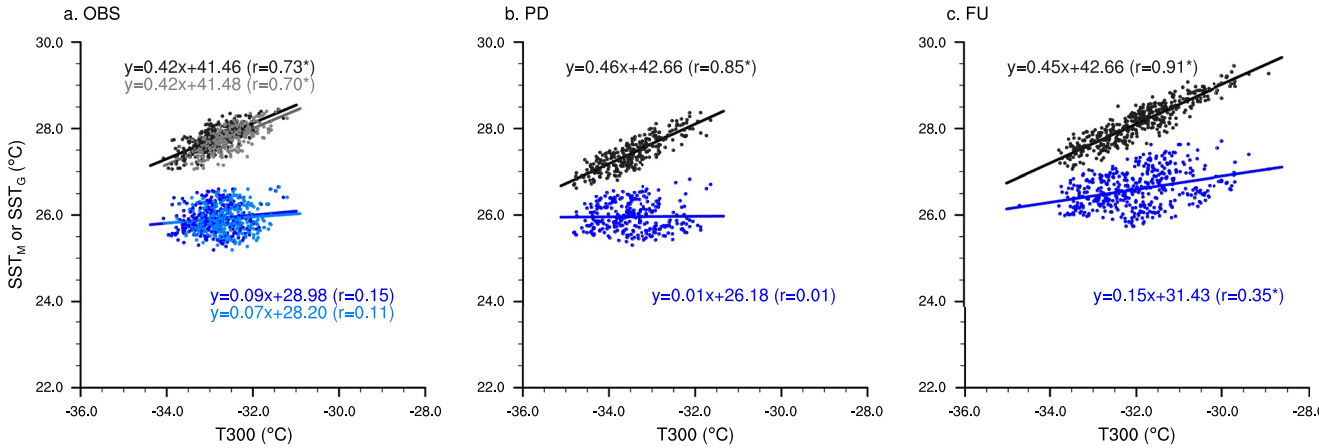

Figure 4. Scatter plot of sea surface temperature (SST) at the genesis of mesoscale convective system (SST_G, black dots) and tropical mean SST (SST_M, blue dots) versus tropical mean upper-tropospheric (300 hPa) temperature (T300) based on (a) observation, (b) C192AM4-PD, and (c) C192AM4-FU. (a and b) cover the period of 1985–2008 while (c) covers the period of 2015–2050. Darker (lighter) dots in (a) denotes results from NCEP-R2 (ERA5). Regression equations and correlation coefficients are shown for each fitting line. Asterisk indicates the correlation coefficient is statistically significant at the 95% confidence level.

over Southeast and Southwest Pacific (Figure 2c). It shares a large similarity with the pattern of mean SST change (Figure S2 in Supporting Information S1). The probability density distribution of SST_G in C192AM4-FU simulation has shifted toward higher values compared to the C192AM4-PD simulation (Figure 1a). Moreover, the upward trend of SST_G is projected to increase at a faster rate of 0.28°C per decade, in sync with the trend of SST_M at the rate of 0.26°C per decade (Figure 3c). The larger rate in SST_M is because of the use of RCP8.5 warming scenario in C192AM4-FU simulation. Similar to the C192AM4-PD simulation, the increase in SST_G in C192AM4-FU is dominated by changes in SST_G^{Env} (Figure 3f).

The strong coupling of SST_G with SST_M has been reported in previous studies (Defforge & Merlis, 2017b; Johnson & Xie, 2010; Sobel et al., 2002), which is argued to be associated with the quasi-uniform change of SST_G relative to SST_M. This is evident in Figure 1b, in which the uniform shift of SST_G between warming and historical simulations has diminished if relative SST_G (SST_G minus tropical mean) is used, indicating that SST_G are projected to change little with respect to the tropical mean SST under global warming. This has been found in TC-related rainfall areas in previous study based on both satellite observation and model simulations (Lin et al., 2015). The spatial distribution of the difference between SST_G and SST_M is projected to stay the same as the current climate (Figure S3c in Supporting Information S1). The ratio between tropical mean SST_G and SST_M is close to 1.1 in both observation and C192AM4-PD simulation and remains almost unchanged as climate warms (Figure S10 in Supporting Information S1). This invariant ratio between SST_G and SST_M suggests little change in the fraction of convectively active areas over the tropical ocean. In practice, the fractional area of tropical ocean exceeding three MCSs per 5° × 5° per month (the tropical mean oceanic MCS genesis number in current climate) has decreased by 2% per degree of global warming (Figure S1 in Supporting Information S1) based on the model simulations, while the fractional area exceeding 26°C SST isotherm has increased by 4% per degree global warming (Figure S2 in Supporting Information S1).

Besides, SST_G is strongly related to tropical upper-tropospheric temperatures considering that the tropical atmosphere is dominated by these saturated convective updrafts (Johnson & Xie, 2010; Sobel et al., 2002). Changes in SST_G could be a useful indicator of the tropospheric temperature changes, which have remained controversial for a long-time due to the non-climatic artifacts found in radiosonde and satellite-derived data sets (Fu et al., 2004; Randel & Wu, 2006; Sherwood et al., 2005). Figure 4 shows the scatter plot between the SST_G and upper-tropospheric (300 hPa) temperature (T300). Remarkable correspondences are noted between SST_G and T300 based on both the ERA5 ($r = 0.70$, $p < 0.001$) and NCEP-R2 ($r = 0.73$, $p < 0.001$). The regression coefficients are 0.42°C per °C for both ERA5 and NCEP-R2 data sets. This relationship is well reproduced by the C192AM4-PD simulations. The simulated regression coefficient is 0.46°C per °C ($r = 0.85$, $p < 0.001$), which remains almost unchanged in the C192AM4-FU simulation (0.45°C per °C, $r = 0.91$, $p < 0.001$). It is not clear to what extent these results might be model dependent, but they are consistent with previous findings based on the theory of moist adiabatic lapse rate adjustment (~0.43°C per °C, Johnson & Xie, 2010). Such a consistency

indicates that the tropical atmosphere will follow a moist adiabat as climate warms to first order. Given the intimate relationship between SST_G and SST_M shown above, one might expect a close correspondence between SST_M and T300. However, much weaker correlation coefficients are noted between SST_M and T300 (Figure 4). This is because SST_M also includes non-convecting regions, in which the SST has no direct way to influence the free troposphere. In this regard, SST_G may provide more important information than the tropical mean SST on tropical tropospheric temperature change. This has been noted and discussed in previous studies (Flannaghan et al., 2014; Fueglistaler et al., 2015), which found that the precipitation-weighted SST, an index that give more weight to SST in regions where it rains more, can partly reconcile observations and simulations of tropical upper tropospheric temperature trends while other factors, like the convection parametrization and associated small-scale processes in the models, are also responsible (Keil et al., 2021). Moreover, the different evolution of tropical mean SSTs and SSTs in regions of deep convection may help to explain the discrepancy between the trends in SST_G and SST_M (Figure 3).

The moist adiabatic lapse rate adjustment, found in both observation and model simulations, suggests an overall reduction in tropical convection with the increase in SST_G since the environment for tropical systems formation, like MCSs, is becoming more stable as climate warms. Such changes manifest as a reduction of the upward mass flux over the convective regions (Held & Soden, 2006), leading to a notable reduction in observed MCSs globally (Dong et al., 2021). At a regional scale, non-uniform SST changes can cause shifts in active convective regions, other factors such as large-scale circulation, internal climate variability and localized aerosol effects can also lead to shifts in those areas of active convection, making it difficult to detect and attribute any long-term changes in regional systems. To put it in a more general context, the temperature of near surface air has to reach a certain threshold for it to rise. As climate warms, the tropical atmosphere follows the moist adiabat and the critical temperature increases along with the surface warming. The upper-tropospheric temperature needs to adjust accordingly to keep up, which in turn creates conditions less favorable for the formation of convection. These arguments have been discussed in many idealized or climate model simulations studying TCs (Chand et al., 2022; Sobel et al., 2021). Recent studies based on observation have shown a decreasing trend of global TC frequency with duration larger than 2 days since 1990 (Klotzbach et al., 2022), while an increase in SST at the genesis of TCs was observed at the same time (Defforge & Merlis, 2017b). Our analysis thus extends the previous study on tropical TCs to more frequently occurring MCSs, providing another piece of evidence that can increase our confidence in future projections of fewer tropical systems associated with global warming.

4. Conclusions

This work is the first study to extend the analysis of the linkage between tropical convection and underlying SST to MCS. The event-based evaluation of SST at the genesis of MCS fills in the gap between pioneer works based on either limitedTCs (~90 per year) or general convection estimated by monthly precipitation data set. The capability of the model in capturing the observed SST_G features suggests it is a useful tool to study future projections. The variability of the tropical SST threshold for MCS genesis is robust and clearly detectable in both observations and the high-resolution C192AM4 model. The tropical mean SST_G is about 28°C in the current climate with a small seasonality. Both observations and the C192AM4-PD simulation show that SST_G has undergone a significant warming trend at a rate of ~0.2°C per decade during their overlapping period of 1985–2008. Moreover, the SST_G shows negligible dependences on the MCS duration and size, but it has a strong dependence on the MCS intensity, with stronger MCS corresponding to larger SST_G. The SST_G trends show no dependence on MCS duration and size, but larger trends are observed for weaker systems. The SST_G shows a remarkable correspondence with the tropical mean SST on interannual and longer timescales. The relative influence of the MCS genesis location changes on the upward trend of SST_G is negligible when compared to the environmental SST warming, which predominantly determines the positive trend of SST_G. A warming simulation projects a continuous increase in SST_G, but a constant relationship between SST_G and upper tropospheric temperature is found in both the current and warming simulations, which confirms the notion that the tropical troposphere has warmed and will continue to warm in a way following the moist adiabatic adjustment. Consequently, we may expect fewer but stronger tropical systems, such as TCs and MCSs, in warming projections.

Conflict of Interest

The authors declare no conflicts of interest relevant to this study.

Data Availability Statement

The brightness temperature data sets from the Cloud Archive User Service (CLAUS) product are available at https://data.ceda.ac.uk/badc/claus/data/. The OISST data can be obtained from https://www.ncei.noaa.gov/data/sea-surface-temperature-optimum-interpolation/v2.1/access/avhrr/. The HadISST data is download from https://www.metoffice.gov.uk/hadobs/hadisst2/. The C192AM4 model outputs can be downloaded from https://esgf-node.llnl.gov/search/cmip6/. The GFDL AM4 model source code can be obtained from https://data1.gfdl.noaa.gov/nomads/forms/am4.0/.

Acknowledgments
The authors would like to thank Nathaniel C. Johnson and Hiroyuki Murakami for useful discussion and commenting on earlier versions of this paper. This research from the Geophysical Fluid Dynamics Laboratory is supported by NOAA's Science Collaboration Program and administered by UCAR's Cooperative Programs for the Advancement of Earth System Science (CPAESS) under awards NA16NWS4620043 and NA18NWS4620043B

References

Chand, S. S., Walsh, K. J. E., Camargo, S. J., Kossin, J. P., Tory, K. J., Wehner, M. F., et al. (2022). Declining tropical cyclone frequency under global warming. *Nature Climate Change*, *12*(7), 655–661. https://doi.org/10.1038/s41558-022-01388-4

Dare, R. A., & McBride, J. L. (2011). The threshold sea surface temperature condition for tropical cyclogenesis. *Journal of Climate*, *24*(17), 4570–4576. https://doi.org/10.1175/jcli-d-10-05006.1

Defforge, C. L., & Merlis, T. M. (2017a). Evaluating the evidence of a global sea surface temperature threshold for tropical cyclone genesis. *Journal of Climate*, *30*(22), 9133–9145. https://doi.org/10.1175/jcli-d-16-0737.1

Defforge, C. L., & Merlis, T. M. (2017b). Observed warming trend in sea surface temperature at tropical cyclone genesis. *Geophysical Research Letters*, *44*(2), 1034–1040. https://doi.org/10.1002/2016gl071045

De Meyer, V., & Roca, R. (2021). Thermodynamic scaling of extreme daily precipitation over the tropical ocean from satellite observation. *Journal of the Meteorological Society of Japan*, *99*(2), 423–436. https://doi.org/10.2151/jmsj.2021-020

Dong, W., Lin, Y., Zhang, M., & Huang, X. (2020). Footprint of tropical mesoscale convective system variability on stratospheric water vapor. *Geophysical Research Letters*, *47*(5), e2019GL086320. https://doi.org/10.1029/2019gl086320

Dong, W., Zhao, M., Ming, Y., & Ramaswamy, V. (2021). Representation of tropical mesoscale convective systems in a general circulation model: Climatology and response to global warming. *Journal of Climate*, *34*(14), 5657–5671. https://doi.org/10.1175/jcli-d-20-0535.1

Doswell, C. A., III, Brooks, H. E., & Maddox, R. A. (1996). Flash flood forecasting: An ingredients-based methodology. *Weather and Forecasting*, *11*(4), 560–581. https://doi.org/10.1175/1520-0434(1996)011<0560:fffaib>2.0.co;2

Evans, J. L., & Waters, J. J. (2012). Simulated relationships between sea surface temperatures and tropical convection in climate models and their implications for tropical cyclone activity. *Journal of Climate*, *25*(22), 7884–7895. https://doi.org/10.1175/jcli-d-11-00392.1

Flannaghan, T. J., Fueglistaler, S., Held, I. M., Po-Chedley, S., Wyman, B., & Zhao, M. (2014). Tropical temperature trends in Atmospheric General Circulation Model simulations and the impact of uncertainties in observed SSTs. *Journal of Geophysical Research: Atmospheres*, *119*(23), 13327–13337. https://doi.org/10.1002/2014jd022365

Fu, Q., Johanson, C. M., Warren, S. G., & Seidel, D. J. (2004). Contribution of stratospheric cooling to satellite-inferred tropospheric temperature trends. *Nature*, *429*(6987), 55–58. https://doi.org/10.1038/nature02524

Fueglistaler, S., Radley, C., & Held, I. M. (2015). The distribution of precipitation and the spread in tropical upper tropospheric temperature trends in CMIP5/AMIP simulations. *Geophysical Research Letters*, *42*(14), 6000–6007. https://doi.org/10.1002/2015gl064966

Graham, N., & Barnett, T. (1987). Sea surface temperature, surface wind divergence, and convection over tropical oceans. *Science*, *238*(4827), 657–659. https://doi.org/10.1126/science.238.4827.657

Haarsma, R. J., Roberts, M. J., Vidale, P. L., Senior, C. A., Bellucci, A., Bao, Q., et al. (2016). High resolution model intercomparison project (HighResMIP v1. 0) for CMIP6. *Geoscientific Model Development*, *9*(11), 4185–4208. https://doi.org/10.5194/gmd-9-4185-2016

Held, I. M., & Soden, B. J. (2006). Robust responses of the hydrological cycle to global warming. *Journal of Climate*, *19*(21), 5686–5699. https://doi.org/10.1175/jcli3990.1

Hersbach, H., Bell, B., Berrisford, P., Hirahara, S., Horányi, A., Muñoz-Sabater, J., et al. (2020). The ERA5 global reanalysis. *Quarterly Journal of the Royal Meteorological Society*, *146*(730), 1999–2049. https://doi.org/10.1002/qj.3803

Houze, R. A., Jr. (2004). Mesoscale convective systems. *Reviews of Geophysics*, *42*(4). https://doi.org/10.1029/2004rg000150

Houze, R. A., Jr. (2018). 100 years of research on mesoscale convective systems. *Meteorological Monographs*, *59*, 17–21. https://doi.org/10.1175/amsmonographs-d-18-0001.1

Huang, X., Hu, C., Huang, X., Chu, Y., Tseng, Y.-h., Zhang, G. J., & Lin, Y. (2018). A long-term tropical mesoscale convective systems dataset based on a novel objective automatic tracking algorithm. *Climate Dynamics*, *51*(7), 3145–3159. https://doi.org/10.1007/s00382-018-4071-0

Johnson, N. C., & Xie, S.-P. (2010). Changes in the sea surface temperature threshold for tropical convection. *Nature Geoscience*, *3*(12), 842–845. https://doi.org/10.1038/ngeo1008

Kanamitsu, M., Ebisuzaki, W., Woollen, J., Yang, S.-K., Hnilo, J., Fiorino, M., & Potter, G. (2002). NCEP-DOE AMIP-II reanalysis (R-2). *Bulletin of the American Meteorological Society*, *83*(11), 1631–1644. https://doi.org/10.1175/bams-83-11-1631(2002)083<1631:nar>2.3.co;2

Keil, P., Schmidt, H., Stevens, B., & Bao, J. (2021). Variations of tropical lapse rates in climate models and their implications for upper-tropospheric warming. *Journal of Climate*, *34*(24), 9747–9761. https://doi.org/10.1175/jcli-d-21-0196.1

Klotzbach, P. J., Wood, K. M., Schreck, C. J., Bowen, S. G., Patricola, C. M., & Bell, M. M. (2022). Trends in global tropical cyclone activity: 1990–2021. *Geophysical Research Letters*, *49*(6), e2021GL095774. https://doi.org/10.1029/2021gl095774

Kossin, J. P. (2015). Validating atmospheric reanalysis data using tropical cyclones as thermometers. *Bulletin of the American Meteorological Society*, *96*(7), 1089–1096. https://doi.org/10.1175/bams-d-14-00180.1

Kunkel, K. E., Easterling, D. R., Kristovich, D. A., Gleason, B., Stoecker, L., & Smith, R. (2012). Meteorological causes of the secular variations in observed extreme precipitation events for the conterminous United States. *Journal of Hydrometeorology*, *13*(3), 1131–1141. https://doi.org/10.1175/jhm-d-11-0108.1

Lin, Y., Zhao, M., & Zhang, M. (2015). Tropical cyclone rainfall area controlled by relative sea surface temperature. *Nature Communications*, *6*(1), 6591. https://doi.org/10.1038/ncomms7591

McCollum, D. M., Maddox, R. A., & Howard, K. W. (1995). Case study of a severe mesoscale convective system in central Arizona. *Weather and Forecasting*, *10*(3), 643–665. https://doi.org/10.1175/1520-0434(1995)010<0643:csoasm>2.0.co;2

McTaggart-Cowan, R., Davies, E. L., Fairman, J. G., Jr., Galarneau, T. J., Jr., & Schultz, D. M. (2015). Revisiting the 26.5°C sea surface temperature threshold for tropical cyclone development. *Bulletin of the American Meteorological Society*, *96*(11), 1929–1943. https://doi.org/10.1175/bams-d-13-00254.1

Moncrieff, M. W. (2004). Analytic representation of the large-scale organization of tropical convection. *Journal of the Atmospheric Sciences*, *61*(13), 1521–1538. https://doi.org/10.1175/1520-0469(2004)061<1521:arotlo>2.0.co;2

Moncrieff, M. W., & Liu, C. (2006). Representing convective organization in prediction models by a hybrid strategy. *Journal of the Atmospheric Sciences*, *63*(12), 3404–3420. https://doi.org/10.1175/jas3812.1

Randel, W. J., & Wu, F. (2006). Biases in stratospheric and tropospheric temperature trends derived from historical radiosonde data. *Journal of Climate*, *19*(10), 2094–2104. https://doi.org/10.1175/jcli3717.1

Rayner, N. A., Parker, D. E., Horton, E. B., Folland, C. K., Alexander, L. V., Rowell, D. P., et al. (2003). Global analyses of sea surface temperature, sea ice, and night marine air temperature since the late nineteenth century. *Journal of Geophysical Research*, *108*(D14), 4407. https://doi.org/10.1029/2002jd002670

Reynolds, R. W., Smith, T. M., Liu, C., Chelton, D. B., Casey, K. S., & Schlax, M. G. (2007). Daily high-resolution-blended analyses for sea surface temperature. *Journal of Climate*, *20*(22), 5473–5496. https://doi.org/10.1175/2007jcli1824.1

Roca, R., Fiolleau, T., & Bouniol, D. (2017). A simple model of the life cycle of mesoscale convective systems cloud shield in the tropics. *Journal of Climate*, *30*(11), 4283–4298. https://doi.org/10.1175/jcli-d-16-0556.1

Sherwood, S. C., Lanzante, J. R., & Meyer, C. L. (2005). Radiosonde daytime biases and late-20th century warming. *Science*, *309*(5740), 1556–1559. https://doi.org/10.1126/science.1115640

Sobel, A. H., Held, I. M., & Bretherton, C. S. (2002). The ENSO signal in tropical tropospheric temperature. *Journal of Climate*, *15*(18), 2702–2706. https://doi.org/10.1175/1520-0442(2002)015<2702:tesitt>2.0.co;2

Sobel, A. H., Wing, A. A., Camargo, S. J., Patricola, C. M., Vecchi, G. A., Lee, C., & Tippett, M. K. (2021). Tropical cyclone frequency. *Earth's Future*, *9*(12), e2021EF002275. https://doi.org/10.1029/2021ef002275

Tompkins, A. M. (2001). On the relationship between tropical convection and sea surface temperature. *Journal of Climate*, *14*(5), 633–637. https://doi.org/10.1175/1520-0442(2001)014<0633:otrbtc>2.0.co;2

Tory, K. J., & Dare, R. A. (2015). Sea surface temperature thresholds for tropical cyclone formation. *Journal of Climate*, *28*(20), 8171–8183. https://doi.org/10.1175/jcli-d-14-00637.1

Zhang, C. (1993). Large-scale variability of atmospheric deep convection in relation to sea surface temperature in the tropics. *Journal of Climate*, *6*(10), 1898–1913. https://doi.org/10.1175/1520-0442(1993)006<1898:lsvoad>2.0.co;2

Zhao, M. (2020). Simulations of atmospheric rivers, their variability, and response to global warming using GFDL's new high-resolution general circulation model. *Journal of Climate*, *33*(23), 10287–10303. https://doi.org/10.1175/jcli-d-20-0241.1

Zhao, M. (2022). A Study of AR-TS-and MCS-associated precipitation and extreme precipitation in present and warmer climates. *Journal of Climate*, *35*(2), 479–497. https://doi.org/10.1175/jcli-d-21-0145.1

Zhao, M., Golaz, J.-C., Held, I., Guo, H., Balaji, V., Benson, R., et al. (2018a). The GFDL global atmosphere and land model AM4. 0/LM4. 0: 1. Simulation characteristics with prescribed SSTs. *Journal of Advances in Modeling Earth Systems*, *10*(3), 691–734. https://doi.org/10.1002/2017ms001208

Zhao, M., Golaz, J.-C., Held, I., Guo, H., Balaji, V., Benson, R., et al. (2018b). The GFDL global atmosphere and land model AM4. 0/LM4. 0: 2. Model description, sensitivity studies, and tuning strategies. *Journal of Advances in Modeling Earth Systems*, *10*(3), 735–769. https://doi.org/10.1002/2017ms001209